

Structural analyses of polymorphic transitions of *sn*-1,3-distearoyl-2-oleoylglycerol (SOS) and *sn*-1,3-dioleoyl-2-stearoylglycerol (OSO): assessment on steric hindrance of unsaturated and saturated acyl chain interactions

Junko Yano,^{1,*} Kiyotaka Sato,^{*} Fumitoshi Kaneko,[†] Donald M. Small,[§] and Dharma R. Kodali^{**}

Faculty of Applied Biological Science,^{*} Hiroshima University, Higashi-Hiroshima, 739-8528 Japan; Department of Macromolecular Science,[†] Graduate School of Science, Osaka University, Toyonaka, 560-0043 Japan; Department of Biophysics,[§] Housman Medical Research Center, Boston, MA 02118; and Central Research,^{**} Cargill Inc., Minneapolis, MN 55440-5699

Abstract Polymorphic transformations in two saturated-unsaturated mixed acid triacylglycerols, SOS (*sn*-1,3-distearoyl-2-oleoylglycerol) and OSO (*sn*-1,3-dioleoyl-2-stearoylglycerol), have been studied by FT-IR spectroscopy using deuterated specimens in which stearoyl chains are fully deuterated. A reversible phase transition between *sub* α and α and a series of irreversible transitions ($\alpha \rightarrow \gamma \rightarrow \beta' \rightarrow \beta$ (β_2, β_1) for SOS and $\alpha \rightarrow \beta' \rightarrow \beta$ for OSO) were studied with an emphasis on the conformational ordering process of stearoyl and oleoyl chains. The $\alpha \rightarrow \textit{sub} \alpha$ reversible transition was due to the orientational change of stearoyl chains in the lateral directions from the hexagonal subcell to a perpendicularly packed one. As the first stage of the series of irreversible transitions from α to β , the conformational ordering of saturated chains took place in the $\alpha \rightarrow \gamma$ transition of SOS and in the $\alpha \rightarrow \beta'$ transition of OSO; one stearoyl chain in SOS and OSO takes the all-*trans* conformation and the second stearoyl chain in SOS takes the bent conformation like those observed in the most stable β -type. As the final stage, the ordering of unsaturated chains occurred in the $\beta' \rightarrow \beta$ transition both for SOS and OSO. A conversion in the layered structure from bilayer to trilayer was also accompanied by the conformational ordering in the $\alpha \rightarrow \gamma$ transition of SOS and in the $\beta' \rightarrow \beta$ transition of OSO.—Yano, J., K. Sato, F. Kaneko, D. M. Small, and D. R. Kodali. Structural analyses of polymorphic transitions of *sn*-1,3-distearoyl-2-oleoylglycerol (SOS) and *sn*-1,3-dioleoyl-2-stearoylglycerol (OSO): assessment on steric hindrance of unsaturated and saturated acyl chain interactions. *J. Lipid Res.* 1999. 40: 140–151.

Supplementary key words polymorphism • phase behavior • infrared spectroscopy • molecular packing • molecular conformation • deuteration

The aliphatic chain-chain interactions are critical factors for the determination of physical properties such as softness and flexibility of the fats and lipids present in bio-tissues. Their packing conditions depend on chemical na-

tures of fatty acid moieties: chain length, parity (odd or even), unsaturation (*cis* or *trans*), etc. Most of the biologically important lipid specimens are composed of saturated and unsaturated acyl chains as revealed in diacylglycerols and phospholipids. Diacylglycerols act as an activator of protein kinase C and a signal transducer in metabolism (1–5). Phospholipids produce fluidity of membrane lipids, often containing a saturated chain in the *sn*-glycerol 1 position and an unsaturated chain in the *sn*-glycerol 2 position (6, 7). Triacylglycerols (TAGs), which are a major metabolic fuel, also consist of saturated and unsaturated acyl chains. Unsaturated acyl moieties have a critical role to prevent the solidification of TAGs; solidification causes lipase activity to be remarkably reduced in poikilothermal animals (8, 9). The presence of these moieties affects melting behavior more effectively than the modification of aliphatic chain length (10).

The aliphatic compounds containing *cis*-unsaturated chains reveal quite diversified polymorphism due to the structural flexibility of olefinic groups. Concerning the *cis*-unsaturated fatty acids, their molecular structures have been unveiled by X-ray diffraction crystal structure analyses and vibrational spectroscopy, IR and Raman (11–16). The molecular structures of *cis*-unsaturated fatty acid esters of cholesterol were also clarified by the use of X-ray diffraction methods (17–19). Through those studies, it has become apparent that the *cis*-olefin group can take various internal-rotation angles in solid states to compensate for the conformational disadvantage, depending on

Abbreviations: TAG, triacylglycerol; SOS, *sn*-1,3-distearoyl-2-oleoylglycerol; OSO, *sn*-1,3-dioleoyl-2-stearoylglycerol; SSS, tristearoylglycerol (C18:0); FT-IR, Fourier transform infrared spectroscopy; ATR, attenuated total reflection; RAS, reflection absorption spectroscopy.

¹To whom correspondence should be addressed.

the balance between the acyl chain length and the double bond position. The mixed-acid TAGs (20–23) and diacylglycerols (24, 25) also exhibited diversified polymorphic behavior, all indicating complicated molecular interactions. The mixing behavior of aliphatic chains is important for understanding the interactions between acyl chains. The miscibility between saturated and unsaturated constituents has been studied in the binary systems of fatty acids and those of TAGs. It was clarified that a saturated constituent was hard to mix with an unsaturated one (26–31). We were interested also in the lateral packing of a TAG containing both saturated and unsaturated acyl chains, which would relate to a significant question of how the saturated and unsaturated chains are accommodated together in biological tissues and industrial products.

In the previous studies on the mixed-acid TAGs of this type, it has been clarified that the steric hindrance between the saturated and unsaturated acyl chains resulted in various metastable phases and a series of polymorphic transformation to the stable phase. From the studies on three kinds of TAGs, Sat-O-Sat (1,3-disaturated-acyl-2-oleoylglycerol) (20, 21), O-Sat-O (1,3-dioleoyl-2-saturated-acylglycerol) (22), and Sat-Sat-O (1,2-disaturated-acyl-3-oleoylglycerol) (23), the following conclusions were obtained. First, the position and quantity of oleoyl groups drastically change polymorphism. For example, SOS (*sn*-1,3-distearoyl-2-oleoylglycerol) shows five polymorphs, α , γ , β' , β_2 , and β_1 , while OSO (*sn*-1,3-dioleoyl-2-stearoylglycerol) shows three polymorphs, α , β' , and β (Figs. 1a, b) (20, 22, 32, 33). Second, there are specific composition ratios for binary systems to form molecular compounds. Concerning this point, the binary systems of SOS/*rac*-1,2-distearoyl-3-oleoylglycerol (SSO) (23), SOS/OSO (28), *sn*-1,3-dipalmitoyl-2-oleoylglycerol (POP)/*sn*-1,3-dioleoyl-2-palmitoylglycerol (OPO) (31), and POP/*rac*-1,2-dipalmitoyl-3-oleoylglycerol (PPO) (30) were investigated. Although each TAG component has different polymorphism, a specific chain-chain interaction caused the formation of the molecular compounds at the 1:1 ratio for each combination.

In this study we aimed to clarify the conformation and lateral packing of the saturated and unsaturated acyl chains in each polymorphic form of SOS and OSO. For this purpose we used vibrational spectroscopy, which is a useful method to investigate the complicated polymorphism and intermolecular interactions on a molecular level. The information about subcell structure and molecular conformation of aliphatic chain can be derived. We have already applied infrared absorption spectroscopy for the polymorphic studies on mixed-acid TAGs such as SOS, POP, POS, and on binary systems of POP/PPO and POP/OPO (34, 35). In the present study, we adopted the following tactics.

For molecular conformation, the progression bands due to the ν_3 branch (CH_2 wagging) modes of polymethylene segments were used as a probe (36–42). The frequencies of these progression bands are so sensitive to the length of all-*trans* hydrocarbon segments that we can derive the information about which acyl chain of a TAG takes a bend conformation (43, 44).

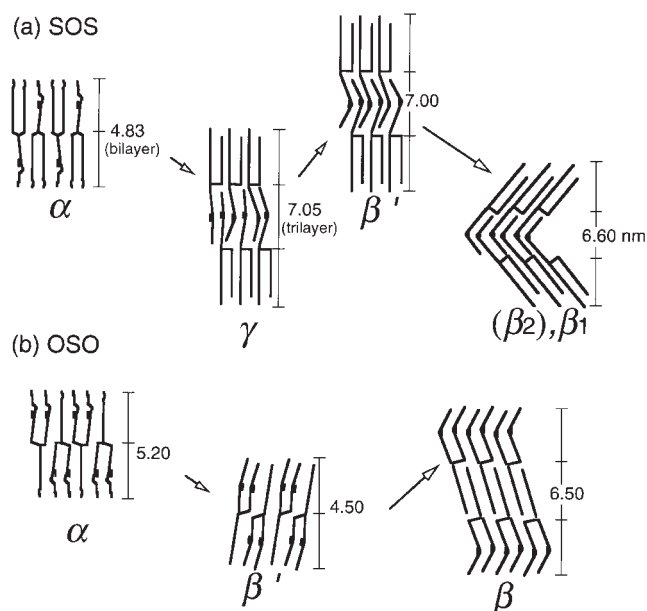


Fig. 1. Schematic representations of polymorphic transformations in (a) *sn*-1,3-distearoyl-2-oleoylglycerol (SOS) and (b) *sn*-1,3-dioleoyl-2-stearoylglycerol (OSO). The models were depicted on the basis of the lamellar distances obtained from the powder X-ray diffraction method and the olefinic group conformations were estimated from the frequencies of the =CH out-of-plane bending mode in IR spectra (20, 22, 32, 33). The α phases of SOS and OSO and the β' phase of OSO pack in bilayer structure, whereas the β' phase of SOS and the β phases of SOS and OSO have the trilayer structure. The lamellar thickness of each polymorph is given.

To get the information about the lateral packing of stearoyl and oleoyl groups separately, we synthesized partially deuterated specimens of SOS and OSO where stearoyl chains are fully deuterated. Using these deuterated specimens, we could avoid the problem of the ordinary hydrogenated specimens (45–47): the overlapping of IR bands due to oleoyl and stearoyl groups. Each group showed IR bands in its own frequency regions due to the mass difference between hydrogen and deuterium.

In this paper, we will demonstrate the utilities of these spectral techniques and show that the conformational ordering of each acyl group is accompanied by an ordering in the lateral packing and/or a structural change in the layer structure.

MATERIALS AND METHODS

Samples

Hydrogenated-SOS (purity >99%) was provided by Fuji Oil Co. Ltd. Hydrogenated-OSO (purity >99%) was purchased from Sigma Co. Ltd. *sn*-1,3-Distearoyl- d_{70} -2-oleoylglycerol and *sn*-1,3-dioleoyl-2-stearoyl- d_{35} -glycerol were synthesized by adopting the methods described in the literature (22, 48) by using perdeuterated stearic- d_{35} acid (obtained from Aldrich Chemical Company) having >98 atom % deuterium.

In this paper we have used the words “d-SOS” and “d-OSO” for the deuterated specimens and “h-SOS” and “h-OSO” for the usual hydrogenated specimens.

Preparation of crystal forms

The following procedures were applied to obtain each polymorphic form both for hydrogenated and deuterated specimens.

SOS. Specimens of the α and γ phases were prepared by holding samples at 80°C for 10 min and then quenching to 10°C and 30°C, respectively (20). A film of the β' phase was made from a chloroform solution on KBr by evaporation method. By holding the β' specimen at 35°C for 8 h, we obtained a film of β (20). As for the two β phases of SOS, we previously concluded that the molecular structures of β_2 and β_1 are almost the same, but the crystal symmetry is different between them (34). As the β_2 -type crystal was not obtained from the deuterated specimen in this study, we focused on the most stable β_1 form of SOS, which is described as β in this paper. Single crystals of the β form were grown from an acetonitrile solution by slow cooling.

OSO. A specimen of the α phase was prepared by quenching a melt to -10°C. By heating the α phases to -5° and 10°C, we obtained specimens of the β' and β phases, respectively (22). Single crystals of the β form were grown from an acetonitrile solution by cooling.

There were a few differences in polymorphic behavior between hydrogenated and deuterated specimens. Each polymorph melted at a slightly lower temperature in a deuterated specimen than in a hydrogenated one, and there was a new metastable phase in d-SOS that melted at a temperature between the melting points of β' (36.5°C) and β_2 (41.0°C). In spite of these differences, there were no significant structural differences between hydrogenated and deuterated specimens. Each polymorph of the deuterated specimens exhibited almost the same X-ray diffraction pattern as that of the hydrogenated specimens.

Powder X-ray diffraction measurements

The X-ray diffraction pattern of each polymorphic form was measured using a Rigaku X-ray diffractometer (40 kV, 10 mA) with Cu-K α radiation. For the measurement at a low temperature, a Rigaku cryostat was used.

Infrared methods

The IR spectra were taken with a Perkin-Elmer Spectrum 2000 spectrometer attached to a Perkin-Elmer ν Series FT-IR microscope. An Oxford flow type cryostat CF1104 and an Oxford temperature controller ITC-4 were used for the measurements at low temperatures. The polarized IR spectra were measured with a MCT detector and a wire-grid polarizer (Perkin-Elmer PR500). The spectra without mention of the conditions were taken at room temperature.

To determine the directions of transition moments three-dimensionally, we used the following three methods of IR measurement.

Polarized IR transmission method. Using single crystal specimens we measured the polarized IR spectra of the β phases with the experimental conditions depicted in Fig. 2a. The incident IR rays impinge normally to the flat face of the crystal. The long crystal edge is set parallel to the direction of $\phi = 90^\circ$.

As the other metastable phases such as γ and β' had difficulty in growing single crystals for the polarized IR measurement, we made a well-oriented film between two KBr windows. The (001) plane of this film is parallel to the KBr window's faces.

The polarization dependence of the IR spectra gives the information about the projections of transition moments onto the (001) plane, i.e., the information is two-dimensional. Therefore, the RAS (reflection absorption spectroscopy) and ATR (attenuated total reflection) methods were necessary in this study.

RAS. For the RAS measurement, a variable angle reflection accessory (Perkin-Elmer) was used. A thin film of TAG was built on a flat aluminum plate by developing a chloroform solution. By

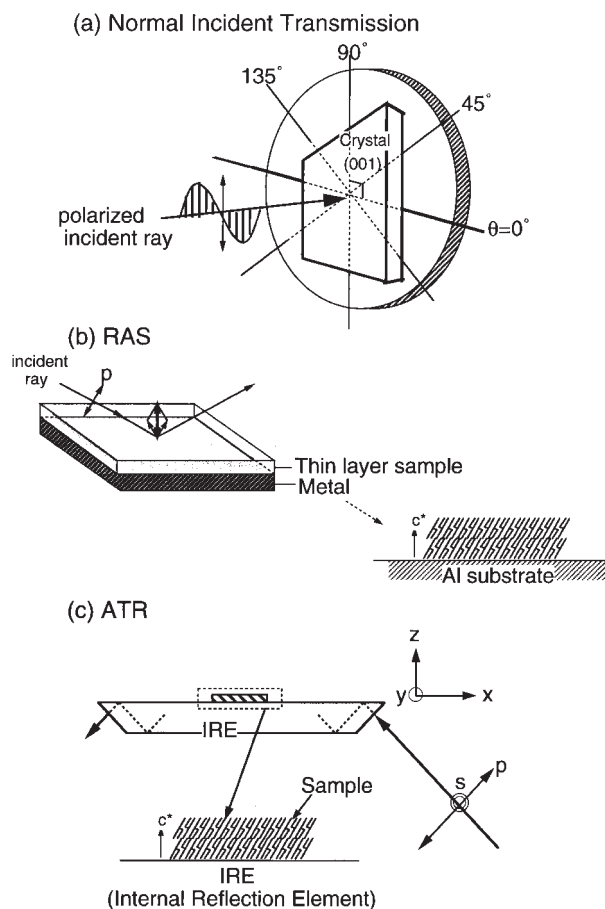


Fig. 2. Schematic representations of (a) the normal incident transmission, (b) RAS, and (c) ATR. In (a), the direction of IR radiation is normal to the (001) plane of the crystal. The direction of the electric field of the incident radiation is fixed and the sample is rotated about the normal of the (001) plane. In (b) and (c), samples were built up on a substrate as a thin film where the lamellar interfaces are parallel to the substrate. With a strong electric field normal to the metal surface, the IR bands having the transition dipole moments normal to the (001) plane are observed selectively in (b). In (c), reflection spectra were measured with p- or s-polarized incident radiation. With p-polarization, the x and z components of a transition moment are observed, and the y component with s-polarization.

controlling the temperature of the substrate, we made a film of each polymorph where the lamellar interfaces are parallel to the metal surface (Fig. 2b). The IR bands whose transition moments are parallel to the chain axis are emphasized with a strong electric field normal to the metal surface (49, 50).

ATR. Polarized ATR spectra were measured using an ATR accessory (PIKE technologies) and a wire-grid polarizer. A Ge plate (wedge angle: 45°) was used as an internal reflection element (IRE). Single crystals or films built on the Ge plate were used as specimens. The x- and z-components of a transition moment are observed with p-polarization, while the y-component is taken with the s-polarization (Fig. 2c) (51).

Assignments of ν_3 progression bands of SSS β

To study the conformation state of stearyl chains in each polymorph of SOS and OSO, the information about the IR bands of tristearoylglycerol (SSS) is important as a reference, in particular the progression bands due to hydrocarbon chains (40, 41, 43).

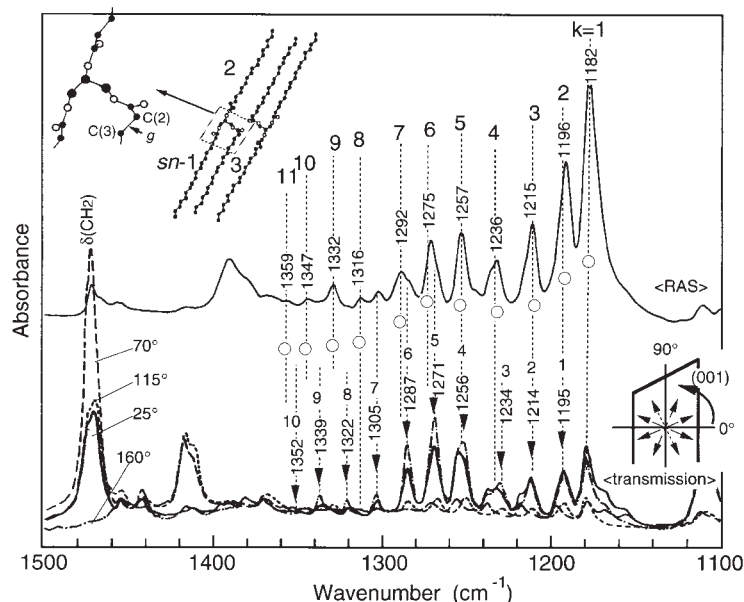


Fig. 3. IR spectra (RAS and normal incident transmission) of SSS β . The molecular structure of SSS is depicted at top left (54–57). Open circles and wedges reveal the ν_3 bands of the *sn*-1,2 straight and *sn*-3 bent stearyl chains, respectively. The frequencies of the ν_3 bands are also given.

The spectral pattern in the region of 1380–1150 cm^{-1} reflects sensitively the stem length of the *trans* zigzag chain. Two series of progression bands overlap in this region, one is due to the ν_3 branch modes (CH_2 wagging: 1360–1150 cm^{-1}) and the other is due to the ν_7 branch modes (CH_2 twisting-rocking: 1300–1150 cm^{-1}) (52, 53). The ν_3 progression bands appear clearly and can be used as a convenient tool.

Figure 3 shows the IR spectra of the β phase of SSS with the band assignments determined in the previous study (43). The bands marked with open circles are of the all-*trans* stearyl chains at the *sn*-1 and *sn*-2 positions, and those with wedges are of the bent stearyl chain at the *sn*-3 position whose C(2)–C(3) bond takes a *gauche* conformation (see top left of Fig. 3) (54–57). The conformational difference has two effects on the ν_3 progression bands. First, the polarization of the ν_3 bands is changed. Because the CH_2 wagging modes of all-*trans* hydrocarbon chains have transition moments parallel to the chain axis, the ν_3 bands of the straight *sn*-1,2 chains clearly appear in RAS. On the other hand, the ν_3 bands of the *sn*-3 chain appear both in the transmission spectra and in the RAS spectra, because the ν_3 modes of the *sn*-3 chain couple with the C–O stretching mode and have both the perpendicular and parallel components to the molecular axis. Second, the *gauche* bond makes these bands shift to higher frequencies as shown in Fig. 3, due to the shortened stem length of the all-*trans* moiety.

RESULTS

α -*sub* α reversible transitions in SOS and OSO

The α phase of monoacid TAGs exhibits a reversible transition to the *sub* α phase (58), but we did not confirm the existence of the *sub* α phase in the previous studies on SOS and OSO.

Figure 4 shows X-ray diffraction patterns of SOS α on cooling. The α form exhibited a single peak of 0.42 nm due to the hexagonal subcell. Below -50°C , this hexagonal subcell seemed to approach gradually to a pseudohexagonal packing having a main peak of 0.42 nm and a

shoulder of 0.38 nm (58). This lower temperature form corresponds to the *sub* α form. The α -*sub* α transition occurred reversibly by temperature changes. We observed this reversible transition also in OSO. The detailed structures of the α and *sub* α phases will be discussed in a later section.

Acyl chain conformation

In order to clarify the conformational changes of each acyl chain during the complex phase transitions of SOS and OSO, we followed the spectral changes in the ν_3 pro-

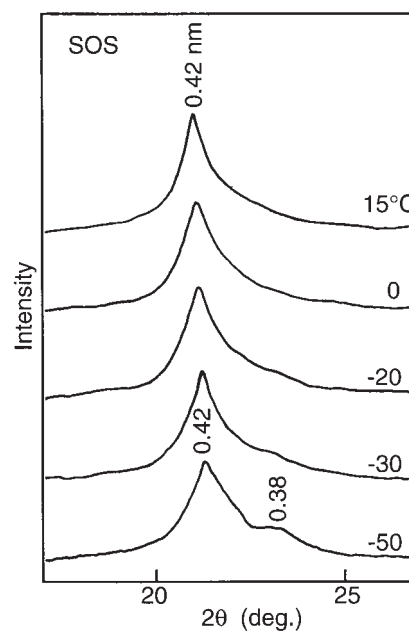


Fig. 4. X-ray diffraction patterns: the changes of XRD patterns during the α -*sub* α transition of SOS. A single peak of 0.42 nm at 15°C is characteristic of the hexagonal packing. As temperature decreased, the hexagonal packing was varied to the pseudohexagonal packing having two peaks of 0.42 and 0.38 nm.

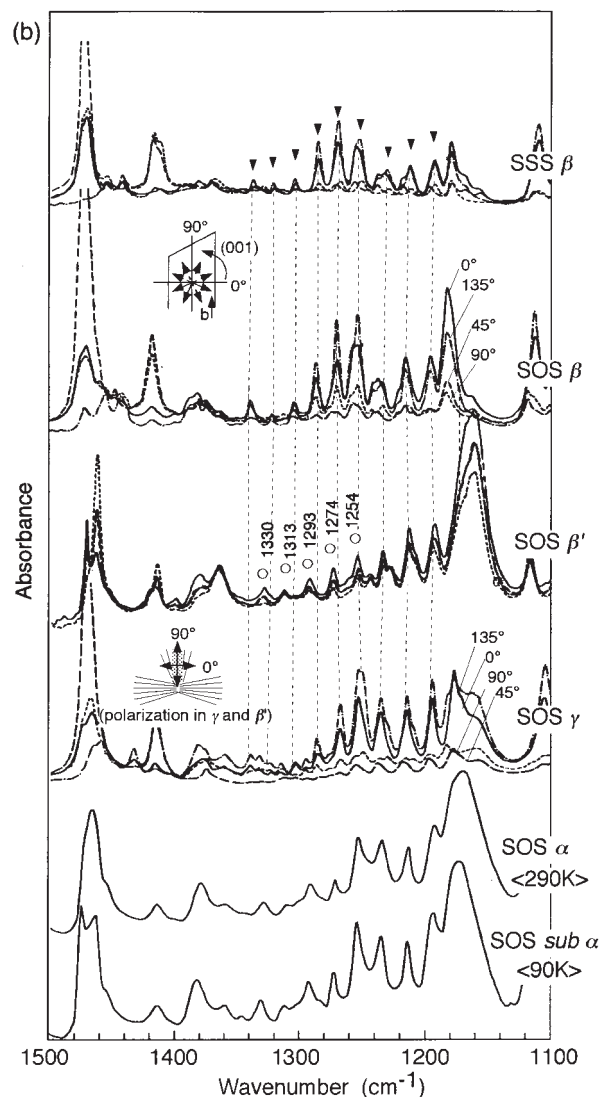
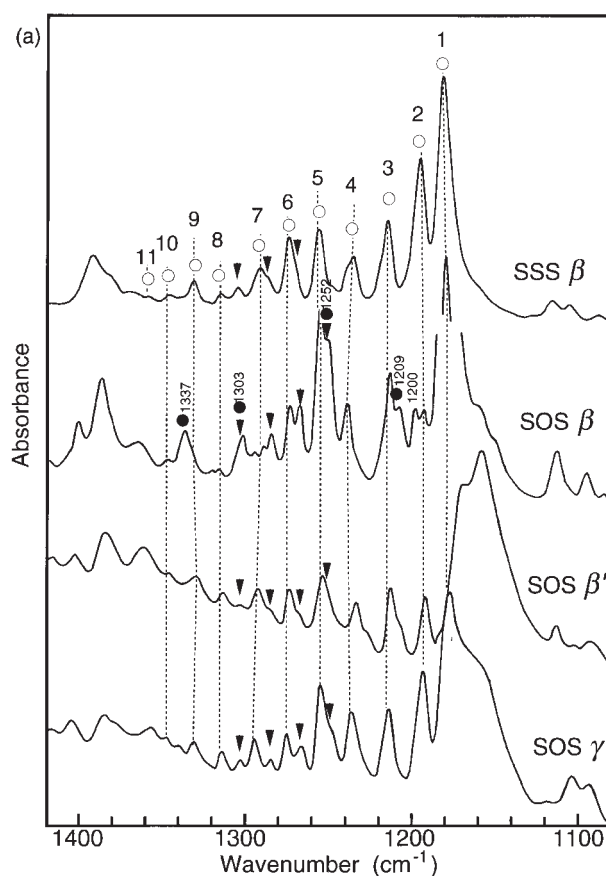


Fig. 5. IR spectra ((a) RAS and (b) normal incident transmission) of h-SOS polymorphs with SSS β . The relationships between the polarization directions and the crystal morphology in the transmission spectra are depicted in (b). In (a) and (b), open circles and wedges show the ν_3 bands of the *sn*-1,2 straight and *sn*-3 bent stearyl chains, respectively. In (a), the bands marked with closed circles in h-SOS β indicate those commonly observed in h-SO β .

gression bands in 1360–1150 cm^{-1} using the normal incident transmission, RAS, and ATR methods.

SOS. Figures 5a, b show the RAS and transmission spectra of each polymorph of h-SOS, in comparison with those of SSS β . The bands marked with open circles in the RAS spectra (Fig. 5a) of SSS β are due to the ν_3 modes of the all-*trans* stearyl chains, while the bands marked with wedges in the transmission spectra (Fig. 5b) of SSS β are due to the ν_3 modes of the bent stearyl chains. Some bands of the bent chain appear also in the RAS spectra (bands marked with wedges).

For all polymorphs of h-SOS, the sharp ν_3 progression bands appeared in their transmission and RAS spectra. The transmission spectra of the α and *sub* α phases exhibited a series of bands whose frequencies are corresponding to those of the all-*trans* stearyl chains. In addition the bands due to the bent stearyl chain were observed in

the RAS and transmission spectra of the γ and β phases. Although the β' phase exhibited only the bands due to the *trans* chain in the transmission spectra, the bands due to the bent chain were certainly confirmed in its RAS spectra. The difference in the polarization of the bent chain's modes between the β' phase and the γ and β phases is presumably related to the orientation of the esterified C–O bond against the zigzag skeletal plane in the bent chain (44).

The 1360–1150 cm^{-1} region of d-SOS provides the information about the conformation of oleoyl group (Fig. 6). There were no sharp oleoyl progression bands in the *sub* α and α spectra. Marked spectral changes were observed through the $\alpha \rightarrow \gamma \rightarrow \beta'$ transition and some sharpened bands were observed in the γ and β' phases. However, only the β phase exhibited a series of bands due to the progression bands of oleoyl group; those bands were

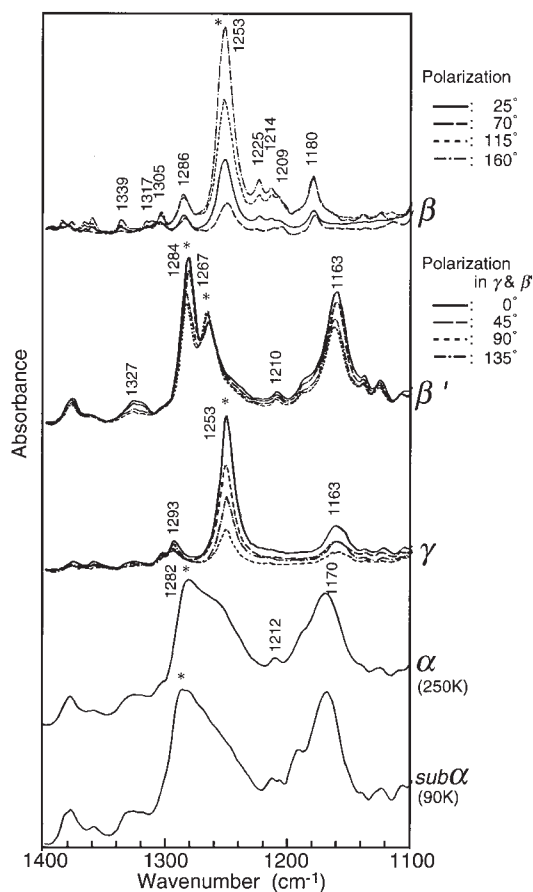


Fig. 6. IR spectra of d-SOS in the 1360–1150 cm^{-1} region. Non-polarized spectra were taken for the *sub* α and α phases and polarized spectra were taken for the γ , β' , and β phases. The bands marked with asterisks show the specific bands observed only in the deuterated specimens. The frequencies of the main bands were also given.

also observed in the RAS spectra (bands marked with closed circles in Fig. 5a).

From the above results we inferred the conformational states of stearoyl and oleoyl groups in each polymorph as follows. In the α and *sub* α phases, stearoyl chains mostly take all-*trans* conformation, yet they contain conformational disorder to a certain extent, while the oleoyl group is conformationally disordered. There is no certain conformational difference between the two stearoyl chains at *sn*-1 and 3 positions. In the γ and β' phases, one of the stearoyl chains changes into a bent conformation, as well as the *sn*-3 chain of SSS; the other stearoyl chain takes the all-*trans* form. Judging from the frequencies of the ν_3 modes, the stearoyl chain takes a *gauche* conformation at the C(2)–C(3) bond of the *sn*-3 chain. The oleoyl group is still in a disordered state. Finally, in the β phase the oleoyl group takes an ordered conformation.

The ordering of the oleoyl group in the β form can be confirmed with a strong IR band of =C–H out-of-plane deformation γ (=C–H) at 688 cm^{-1} , which suggests an ordered *skew-cis-skew'* type conformation of the –C–C=C–C–portion (34). This also indicated that both the methyl-side

(the chain segment between an olefinic group and a CH_3 group) and glycerol-side oleoyl chains (the segment between an olefinic group and a glycerol group) have the all-*trans* conformation.

The conclusions derived from IR spectral changes were consistent with the results of the previous study with Raman spectroscopy (59).

OSO. We used the polarized transmission and the polarized ATR methods for the evaluation of acyl chain conformations in each polymorph (Figs. 7a, b).

Contrary to the IR spectra of SOS β , it seemed that the main spectral features of the transmission spectra in the 1360–1150 cm^{-1} region of h-OSO β came from the two oleoyl groups, as the observed bands totally corresponded to those of d-OSO β (Fig. 8). On the other hand, the ν_3 bands due to the stearoyl group clearly appeared in p-polarized ATR spectra where the modes along the chain axis are intensified, as indicated by open circles in Fig. 7a. These frequencies corresponded to those of the all-*trans* stearoyl chain. Because of experimental difficulties, we could measure ATR spectra only for the β phase. However, the ν_3 bands of the all-*trans* stearoyl chain were observed also in the transmission spectra of the *sub* α , α , and β' phases (Fig. 7b).

As to the oleoyl groups, there were no sharp progression bands in the 1360–1150 cm^{-1} region of d-OSO α and *sub* α phases (Fig. 8). The β' phase exhibited some spectral changes, such as intensity increase, sharpening, and splitting in the 1280–1250 and 1210–1195 cm^{-1} regions. Eventually several sharp progression bands due to oleoyl groups were confirmed in the β phase.

From the above spectral changes, it was inferred that on the phase transitions from α to β , the ordering of the acyl groups proceeds in the following ways. In the α and *sub* α phases, oleoyl chains are disordered but stearoyl chains take the all-*trans* form at a high ratio. The ordering of oleoyl groups takes place to some extent in the β' phase, and in the β phase both stearoyl and oleoyl groups take ordered conformations.

Concerning the conformation around the *cis*-olefin group, a sharp band of =C–H out-of-plane bending γ (=C–H) mode appears at 690 cm^{-1} in β (not shown here). We consider that the olefin groups of the two oleoyl chains take the *skew-cis-skew'* type configuration as in the β phase of SOS (34). On the other hand, there were no detectable γ (=C–H) bands in the region of 730–600 cm^{-1} of the *sub* α , α , and β' phases, which suggests conformational disordering of the olefin group in these three phases.

Chain-chain interactions in lamella

Infrared CH_2 scissoring and CH_2 rocking regions are good indicators of lateral packing, i.e., subcell packing (60). However, the bands of oleoyl groups overlap with those of stearoyl groups for the usual hydrogenated specimens. To get information of individual groups separately, partial deuteration is a useful method (45–47). Deuterated acyl groups show the CD_2 scissoring δ (CD_2) and CD_2 rocking ρ (CD_2) bands around 1090 and 525 cm^{-1} , instead

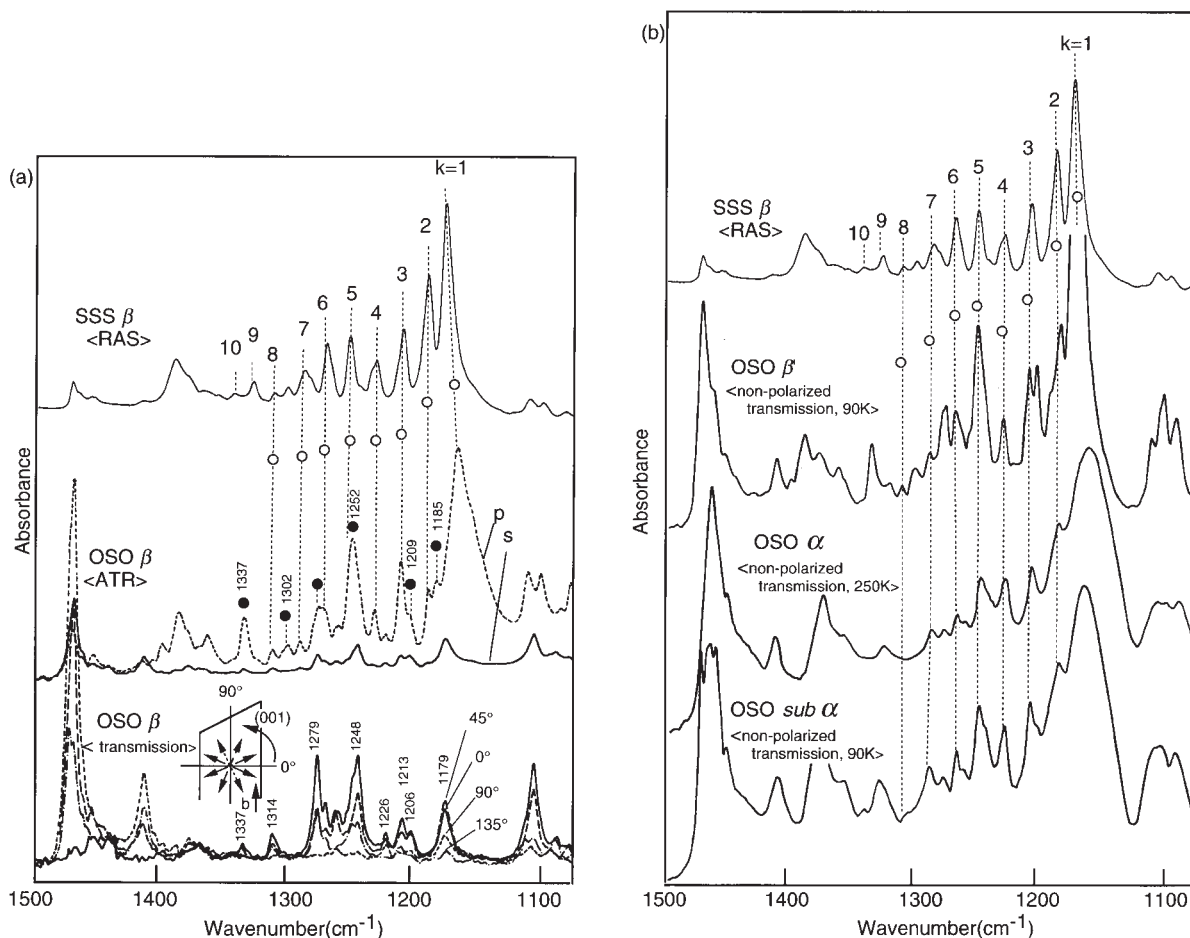


Fig. 7. Comparisons of (a) OSO β spectra (polarized transmission and ATR) with SSS β spectrum (RAS) and (b) OSO $sub\ \alpha$, α , and β' spectra (non-polarized transmission) with SSS β spectrum (RAS). Open circles show the ν_3 bands of the sn -1,2 straight stearyl chains. Closed circles in (a) show the common bands observed in SOS β (Fig. 5a). The frequencies of the main bands were also given. The β' spectrum was taken at a low temperature to avoid the transition to β and also to make the peak positions clear.

of the $\delta(CH_2)$ and $r(CH_2)$ bands around 1460 and 720 cm^{-1} , respectively. For the d-SOS and d-OSO specimens where only stearyl groups are fully deuterated, we can monitor the packing of oleoyl and stearyl groups from the $\delta(CH_2)$ and $\delta(CD_2)$ bands.

In this study, we focused on the spectral changes of the $\delta(CH_2)$ and $\delta(CD_2)$ regions (Figs. 9a, b and Figs. 10a, b), because the frequency of the $r(CD_2)$ mode is too low to be detected with the MCT detector equipped with our spectrometer. Here, the symbols of $\delta(CH_2)o$ and $\delta(CD_2)s$ mean the $\delta(CH_2)$ mode of hydrogenated oleoyl chains and the $\delta(CD_2)$ of deuterated stearyl chains in partially deuterated specimens.

SOS. In the α form, a single $\delta(CH_2)$ band appeared at 1467 cm^{-1} , indicating the hexagonal subcell (Fig. 9a). The $\delta(CH_2)$ band split into two components by cooling, and the splitting width increased as temperature decreased. At 87K the two components were observed at 1474 and 1463 cm^{-1} . In the α form of d-SOS, a single band was observed at 1467 cm^{-1} for $\delta(CH_2)o$ and at 1089 cm^{-1} for $\delta(CD_2)s$ (Fig. 10a), corresponding to the hexagonal subcell (34). On the transformation from α

to $sub\ \alpha$, the $\delta(CD_2)s$ band split into two components at 1093 and 1084 cm^{-1} , while no marked changes occurred in the $\delta(CH_2)o$ band. The splitting of the $\delta(CD_2)s$ band can be attributed to the interchain vibrational coupling between laterally adjoining perdeuterated chains: the in-phase and the out-of-phase vibrations of the two chains (59). Such a splitting of the $\delta(CH_2)$ band has been observed in many systems of long-chain molecules where hydrocarbon chains form a perpendicular type subcell to a certain extent. We inferred that the orientational changes of stearyl chains containing somewhat conformational disorders from the hexagonal to the pseudohexagonal packing take place on the α - $sub\ \alpha$ transition.

The previous study by powder X-ray diffraction method revealed that the γ phase takes a trilayer structure (20), which means that the stearyl and oleoyl moieties make their own leaflet. The $\delta(CH_2)$ band had two components (Fig. 9a) for h-SOS; one strong band at 1472 cm^{-1} and another weak band at 1467 cm^{-1} . Because the former band disappeared in the polarized spectra of d-SOS, we assigned this band to the stearyl scissoring mode and the latter band to the oleoyl scissoring mode (Fig. 10a). A

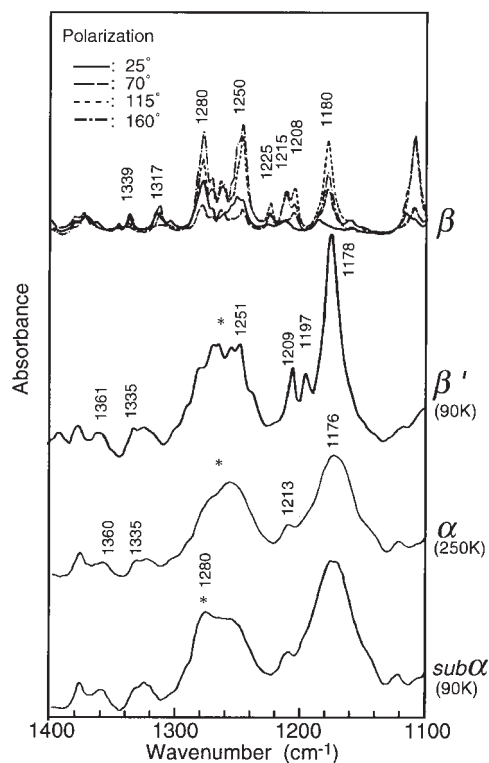


Fig. 8. IR spectra of d-OSO in the 1360–1150 cm^{-1} region. Non-polarized spectra were taken for the *sub* α , α , and β' phases and polarized spectra were taken for the β phase. The bands marked with an asterisk show the specific bands observed only in the deuterated specimens.

sharp single band of $\delta(\text{CD}_2)_s$ appeared at 1092 cm^{-1} , while a broad band of $\delta(\text{CH}_2)_o$ was observed at 1468 cm^{-1} . It is suggested that the stearyl groups form a parallel packing and the oleoyl moiety packs in the hexagonal subcell (60).

In the β' form, the $\delta(\text{CH}_2)$ band had two components, 1473 and 1465 cm^{-1} (Fig. 9a) and the $\delta(\text{CD}_2)_s$ mode split into two components at 1091 and 1088 cm^{-1} (Fig. 10a). Although the polarization directions of the $\delta(\text{CD}_2)_s$ bands were not clear due to the overlapping of other modes, they showed the following characteristics: the 1092 and 1086 cm^{-1} became maximum at the 0° and 90° polarization directions, respectively. These spectral data indicate the $\text{O}\perp$ subcell of the stearyl leaflets (60). This splitting width of the $\delta(\text{CD}_2)_s$ bands (6.5 cm^{-1}) was smaller than that of the typical $\text{O}\perp$ subcell (7.8 cm^{-1}) of deuterated *n*-alkanes (61), suggesting that the packing of the stearyl chains is not so tight as that of *n*-alkanes. The glycerol backbone probably hinders stearyl groups being packed tightly. As to the oleoyl leaflet, the $\delta(\text{CH}_2)_o$ mode became slightly sharper in β' than in γ , but its frequency was still 1468 cm^{-1} , suggesting a lateral packing similar to the hexagonal subcell in α .

In the β form of h-SOS, the single $\delta(\text{CH}_2)$ band appeared at 1470 cm^{-1} with a clear polarization nearly parallel to the b-axis (Fig. 9a); maximum at $\theta = 70^\circ$ and minimum at $\theta = 160^\circ$. The $\delta(\text{CH}_2)_o$ and $\delta(\text{CD}_2)_s$ bands of d-SOS were also observed as single bands at 1471 and 1092 cm^{-1} with a clear polarization (Fig. 9a). The $\delta(\text{CH}_2)_o$ bands appeared at a higher frequency than in the β' form. The results suggested that both the stearyl and oleoyl moieties were packed in $\text{T}'//$ subcell (34).

OSO. In the α forms of h-OSO and d-OSO, single methylene scissoring bands appeared as follows: the $\delta(\text{CH}_2)$ band of h-OSO at 1467 cm^{-1} and the $\delta(\text{CH}_2)_o$ and $\delta(\text{CD}_2)_s$ bands of d-OSO at 1467 and 1089 cm^{-1} (Figs. 9b, 10b), showing the hexagonal packing of acyl chains. In the *sub* α form of h-OSO, three components of the $\delta(\text{CH}_2)$ modes were observed: 1474, 1467, and 1463 cm^{-1} (Fig. 9b). The comparison of these bands with those of d-OSO *sub* α showed that two outer bands at 1474 and 1463

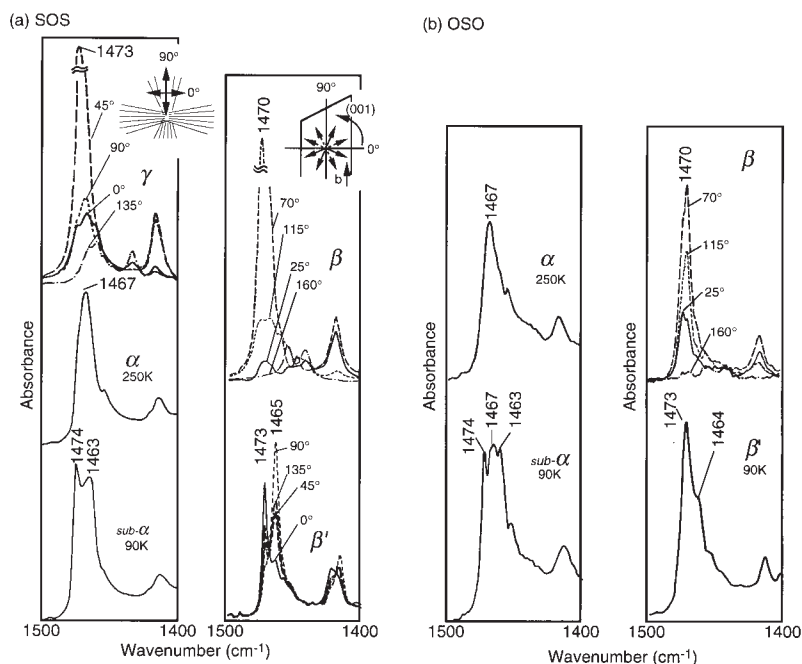


Fig. 9. The $\delta(\text{CH}_2)$ bands of hydrogenated (a) SOS and (b) OSO. Non-polarized spectra were taken for the *sub* α and α phases of SOS and OSO and the β' phase of OSO. For the γ and β' phases of SOS, polarized spectra were taken by the well-oriented specimens as depicted in the top left in (a). For the β phases of SOS and OSO, polarized spectra were taken by the single crystals as depicted in the top right in (a).

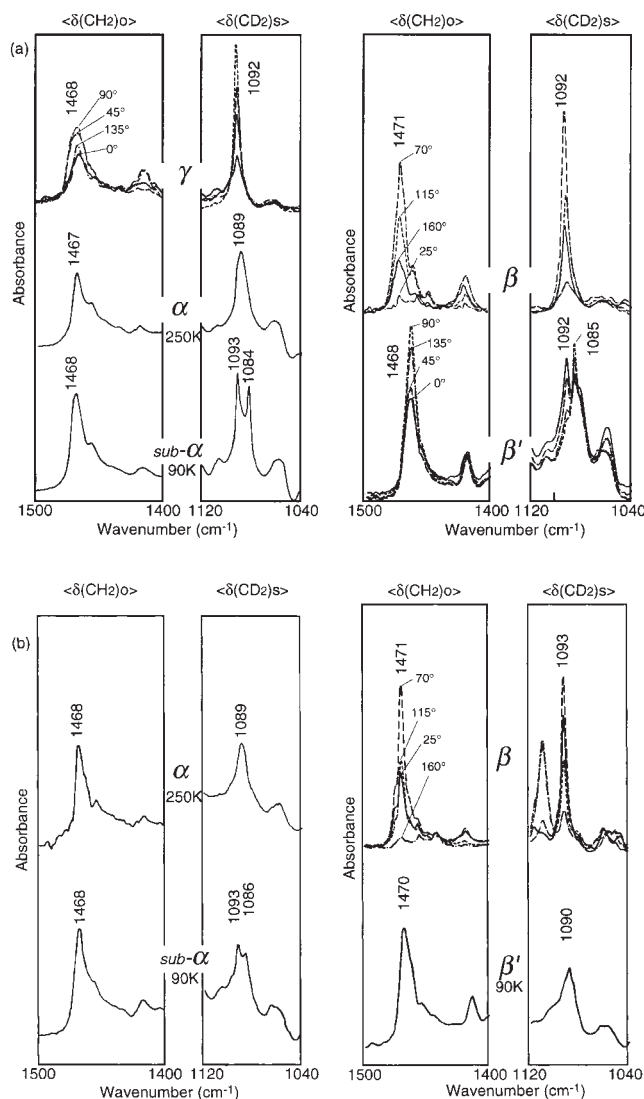


Fig. 10. The $\delta(\text{CH}_2)\text{o}$ and $\delta(\text{CD}_2)\text{s}$ bands of deuterated (a) SOS and (b) OSO. The spectra of each polymorph were measured in the same conditions (temperature and polarization) as stated in Fig. 9.

cm^{-1} are the scissoring doublet arising from pseudohexagonal packing of stearoyl chains and the central band at 1467 cm^{-1} is of the hexagonal packing of oleoyl chains. We concluded that the α - $\text{sub}\alpha$ transition of OSO is associated with the orientational changes of the stearoyl chains from the hexagonal to the pseudohexagonal packing as that of SOS.

Contrary to the trilayer structure of SOS β' , OSO β' takes the bilayer structure (22). In Fig. 9b, the $\delta(\text{CH}_2)$ modes of h-OSO β' had two components: a main component of 1473 cm^{-1} and a shoulder of 1464 cm^{-1} . This asymmetric doublet shows the existence of the $\text{O}\perp$ packing, supporting the result of the powder XRD measurement (22). On the other hand, both the $\delta(\text{CH}_2)\text{o}$ and $\delta(\text{CD}_2)\text{s}$ modes in the deuterated specimen appeared as single bands at 1470 and 1090 cm^{-1} , indicating a parallel-type subcell packing (Fig. 10b). In the deuterated speci-

men, the interchain vibrational coupling between laterally adjoining stearoyl and oleoyl chains can be neglected due to the mass difference. Therefore, the above results suggest the following features: 1) the hydrocarbon skeletal planes of the neighboring stearoyl and oleoyl chains are oriented perpendicularly, but 2) the skeletal planes of the nearest neighboring stearoyl chains are located parallel to each other and those of the neighboring oleoyl chains are also parallel between them. The details will be discussed later.

In the β form, the methylene scissoring modes showed the same clear polarization and positions of bands as those of SOS β . It suggested that both the stearoyl and oleoyl moieties pack in T// subcell (60).

DISCUSSION

Reversible α - $\text{sub}\alpha$ transition

In the SOS bilayer structure, the oleoyl chain is surrounded by the stearoyl chains. These two chains pack together to form the hexagonal subcell in the α phase as illustrated in Fig. 11a. As for the molecular structure of SOS α , the previous ^{13}C CP/MAS-NMR studies indicated the following two properties: 1) in the oleoyl chains two carbons of the *cis* double bond are equivalent and 2) the methyl end packing of stearoyl and oleoyl chains in a molecule are identical (62). On the basis of the assignments of the CH_2 progression bands together with the above results, we infer the molecular structure of α as follows: the stearoyl chains mostly form the extended conformation but contain conformational disorder at their methyl terminals, whereas the oleoyl chain contains disordered conformation with high concentration. The thermal fluctuation of the disordered portions in α is reduced with a decrease in temperature. Consequently, the orientational anisotropy of the neighboring stearoyl chains occurs at the α - $\text{sub}\alpha$ transition due to the thermal contraction. By contrast, the oleoyl chain in $\text{sub}\alpha$ maintains the disordered orientation of the skeletal planes even at low temperatures. As marked differences were not observed between the α and $\text{sub}\alpha$ spectra except for the methylene scissoring modes of the stearoyl chains, we conclude that the α - $\text{sub}\alpha$ transition corresponds only to the orientational changes of the stearoyl chains.

In the OSO bilayer structure, each stearoyl chain is surrounded by the oleoyl chains (Fig. 11b). As stated previously, the molecular structure of stearoyl and oleoyl chains in α and $\text{sub}\alpha$ of OSO is basically the same as those of SOS. Although the intermolecular interaction between the nearest neighboring stearoyl chains is weak, the same orientational anisotropy of the nearest stearoyl chains as that of SOS occurred on the α - $\text{sub}\alpha$ transition of OSO.

The reversible transitions similar to the α - $\text{sub}\alpha$ transitions in SOS and OSO have been observed in other long-chain molecules; for example, Rotator I-Rotator II transition in *n*-alkanes (63-65). These transitions are caused by the orientational changes of the neighboring hydrocar-

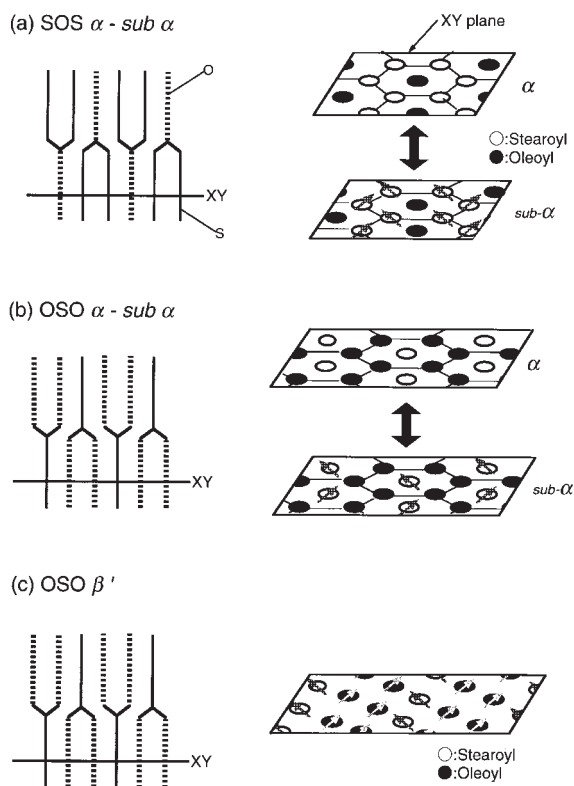


Fig. 11. Schematic representations of the $\alpha \leftrightarrow \text{sub } \alpha$ transitions in SOS (a) and OSO (b) and the acyl chain arrangement of OSO β' (c). Left side reveals the bilayer structure in which the stearoyl and oleoyl chains are indicated by the solid and dotted lines, respectively. Right side shows the chain arrangement in lamella. Open circles and closed circles show the stearoyl and oleoyl chain positions in the XY plane.

bon chains with low energy of activation. Compared with α through β transitions in SOS and OSO having the monotropic nature (66), the α - $\text{sub } \alpha$ transitions take place reversibly, as well as the Rotator II (hexagonal)-Rotator I (pseudo-hexagonal) transition of *n*-alkanes. Such enantiotropic transitions observed in the higher entropy phases may be due to the characteristics common to the highly disordered hydrocarbon chain assemblies. The orientational ordering of the stearoyl chains with decreasing temperature in the $\text{sub } \alpha$ phases of SOS and OSO results in the reduction of the entropy factor, and thereby the enantiotropic transformation occurs between α and $\text{sub } \alpha$.

Another interesting phenomenon from the biological view point is that the fluctuation of the oleoyl chains is retained even at lower temperatures due to the steric hindrance of the olefinic bond. This must be an important character of unsaturated acyl moieties, to maintain the fluidity in biomembrane lipids.

Irreversible transition from α through β forms

The layered structures and the subcell packings of the stearoyl and oleoyl moieties in each polymorphic form of SOS and OSO were summarized in **Table 1**.

In SOS, the α to γ transition is initiated by the stabilization of the stearoyl moieties. Correspondingly, the α form

TABLE 1. Chain-length structure and the subcell packing

Polymorphic Form	Layered Structure	Subcell Structure	
		Stearoyl-Leaflet	Oleoyl-Leaflet
		<i>nm</i>	
SOS			hexagonal
α	double	4.83	
γ	triple	7.05	//-type
β'	triple	7.00	O \perp
(β_2) ^a	triple	6.75	T//
β_1	triple	6.60	T//
OSO			hexagonal
α	double	5.20	(O \perp)
β'	double	4.50	
β	triple	6.50	T//

^aResult from ref. 34.

having bilayer structure transforms to the γ form having trilayer structure. The molecular conformation of the stearoyl chains in γ takes the same ordered conformation as those of more stable β' and β forms in which one chain extends to form the all-*trans* conformation, whereas the other takes a bent conformation in the neighborhood of the ester bond. These stearoyl chains take a parallel type subcell in γ and change to O \perp subcell in β' , but the oleoyl leaflet maintains the hexagonal packing in γ and β' . Although the subcell structure is the same in α and β' , the molecular conformations of the oleoyl chain are different, judging from the spectral features of the oleoyl progression bands in the 1350–1150 cm^{-1} region (Fig. 6). In addition, the NMR studies showed that the methyl-side and the glycerol-side of the oleoyl chain in SOS are not conformationally equivalent in γ and β' unlike in α (62). We infer that the *gauche* bonds in the oleoyl chain are concentrated in the vicinity of the methyl-side chain in the γ and β' phases and are relatively delocated in the α and $\text{sub } \alpha$ phases. The structural difference of the oleoyl chain between γ and β' is probably due to the difference in the concentration of *gauche* bonds. Finally, the β' to β transition corresponds to the stabilization of the oleoyl leaflet where the methyl side-chain and glycerol side-chain take an extended structure with the *skew-cis-skew'* olefinic conformation (34).



In OSO, the α to β' transition corresponds to the stabilization of the stearoyl moiety. Unlike SOS, it was not accompanied by the conversion of the layered structure. As the OSO molecule contains one stearoyl chain, the steric hindrance between the stearoyl and oleoyl chains by the ordering of the stearoyl moiety may not be significant at the initial stage of the phase transition. In the β' phase, the stearoyl chain takes the all-*trans* conformation, whereas the oleoyl chains contain some disordered portions. The sharpened oleoyl bands on the α to β' transition (Fig. 8) showed the progress of the conformational ordering in the oleoyl moieties. On the other hand, unclear methyl rocking bands ($\nu(\text{CH}_3)_o$, usually observed in 950–850 cm^{-1}) suggest the conformational disorder in the methyl end group. We infer that the oleoyl chain conformation in OSO β' is similar to that in SOS β' : the glycerol side-chain takes an extended conformation, but the methyl side-chain contains a certain disorder. Figure 11c is the schematic representation

of the subcell packing of OSO β' . The skeletal zigzag planes of the neighboring stearyl and oleoyl chains are oriented perpendicularly. On the other hand, the zigzag planes of the nearest neighboring stearyl chains and those of the neighboring oleoyl chains are located parallel to each other. The unclear doublet of the $\delta(\text{CH}_2)$ modes (Fig. 9b) compared with that of SOS β' (Fig. 9a) can be explained by the above subcell structure due to the following two points.

First, when the perpendicular and parallel packings coexist in the crystal unit as depicted in Fig. 11c, the former contributes to the band intensity at 1473 and 1464 cm^{-1} and the latter at 1473 cm^{-1} . Therefore, the higher frequency component becomes stronger than the lower one.

Second, when the all-*trans* stearyl chains and the partially disordered oleoyl chains are adjacent to each other, it is difficult to construct a tightly packed subcell.

As the acyl chains tightly pack together, the effect of the steric hindrance between the stearyl and oleoyl chains becomes large; it may result in the conversion of the layered structure from bilayer to trilayer. The final conformation on the polymorphism is basically the same as that of SOS; the β phase forms the trilayer structure where the stearyl and oleoyl chains make their own leaflet as illustrated in Fig. 1b.

The present findings provide molecular level clarification of steric hindrance between the saturated and unsaturated acyl chain in fats and lipids having layered structures. This steric hindrance results in the occurrence of various metastable phases and complicated polymorphic transformations. In the TAG polymorphism having the monotropic characteristics, the transition from the least stable form through the most stable one can be regarded as a process of the crystal growth in solid state. The saturated acyl chains transform to a stable molecular conformation at the first stage of polymorphism and then the unsaturated moieties are stabilized successively with the changes of the subcell structure. The interfacial energy of the stable polymorph is larger than those of the least stable or metastable forms. Namely, the crystallization rates are always higher in the less stable forms and the formation of the stable molecular conformation from melt is sterically hindered.  

Manuscript received 4 May 1998 and in revised form 14 September 1998.

REFERENCES

- Berridge, M. J., and R. F. Irvine. 1984. Inositol triphosphate, a novel second messenger in cellular signal transduction. *Nature* **312**: 315–321.
- Nishizuka, Y. 1984. The role of protein kinase C in cell surface signal transduction and tumor promotion. *Nature* **308**: 693–698.
- Rando, R. R., and N. Yong. 1984. The stereospecific activation of protein kinase C. *Biochem. Biophys. Res. Commun.* **122**: 818–823.
- Seker, M. C., and L. E. Hokin. 1986. The role of phosphoinositides in signal transduction. *J. Membr. Biol.* **89**: 193–210.
- Ganong, B. R., C. R. Loomis, Y. A. Hannun, and R. M. Bell. 1986. Specificity and mechanism of protein kinase C activation by *sn*-1,2-diacylglycerols. *Proc. Natl. Acad. Sci. USA* **83**: 1184–1188.
- Small, D. M. 1984. Lateral chain packing in lipids and membranes. *J. Lipid Res.* **25**: 1490–1500.

- Wang, G., H. Lin, S. Lin, and C. Huang. 1995. Phosphatidylcholines with *sn*-1 saturated and *sn*-2 *cis*-monounsaturated acyl chains. Their melting behavior and structures. *J. Biol. Chem.* **270**: 22738–22746.
- Sugiura, M., and M. Isobe. 1975. Studies on the lipase of *Chromobacterium viscosum*. IV. Substrate specificity of a low molecular weight lipase. *Chem. Pharm. Bull.* **23**: 1226–1230.
- Ohtsu, T., C. Katagiri, M. T. Kumura, and S. H. Hori. 1993. Cold adaptations in drosophila. Qualitative changes of triacylglycerols with relation to overwintering. *J. Biol. Chem.* **268**: 1830–1834.
- Kodali, D. R., D. Atkinson, and D. M. Small. 1989. Molecular packing in triacyl-*sn*-glycerols: influences of acyl chain length and unsaturation. *J. Dispersion Sci. Technol.* **10**: 393–440.
- Abrahamsson, S., and I. Ryderstad-Nahringbauer. 1962. The crystal structure of the low-melting form of oleic acid. *Acta Crystallogr.* **15**: 1261–1268.
- Kobayashi, M., F. Kaneko, K. Sato, and M. Suzuki. 1986. Vibrational spectroscopic study on polymorphism and order-disorder phase transition in oleic acid. *J. Phys. Chem.* **90**: 6371–6378.
- Kaneko, F., K. Yamazaki, K. Kitagawa, T. Kikyo, M. Kobayashi, Y. Kitagawa, Y. Matsuura, K. Sato, and M. Suzuki. 1997. Structure and crystallization behavior of the β phase of oleic acid. *J. Phys. Chem. B* **101**: 1803–1809.
- Kaneko, F., K. Yamazaki, M. Kobayashi, Y. Kitagawa, Y. Matsuura, K. Sato, and M. Suzuki. 1996. Mechanism of the $\gamma \rightarrow \alpha$ and $\gamma 1 \rightarrow \alpha 1$ reversible solid-state phase transitions of erucic acid. *J. Phys. Chem.* **100**: 9138–9148.
- Kaneko, F., M. Kobayashi, K. Sato, and M. Suzuki. 1997. Martensitic phase transition of petroselinic acid: Influence of polytypic structure. *J. Phys. Chem.* **101**: 285–292.
- Sato, K., J. Yano, I. Kawada, M. Kawano, F. Kaneko, and M. Suzuki. 1997. Polymorphic behavior of gondoic acid and phase behavior of its binary mixtures with asclepic acid and oleic acid. *J. Am. Oil Chem. Soc.* **74**: 1153–1160.
- Craven, B. M., and N. G. Guerina. 1979. The crystal structure of cholesteryl oleate. *Chem. Phys. Lipids* **29**: 91–98.
- Craven, B. M., and P. Sawzik. 1983. Conformation and packing of unsaturated chains in cholesteryl linolealdate at 123 K. *J. Lipid Res.* **24**: 784–789.
- Gao, Q., and B. M. Craven. 1986. Conformation of the oleate chains in crystals of cholesteryl oleate at 123 K. *J. Lipid Res.* **27**: 1214–1221.
- Sato, K., T. Arishima, Z. H. Wang, K. Ojima, N. Sagi, and H. Mori. 1989. Polymorphism of POP and SOS. I. Occurrence and polymorphic transformation. *J. Am. Oil Chem. Soc.* **66**: 664–674.
- Arishima, T., N. Sagi, H. Mori, and K. Sato. 1991. Polymorphism of POS. I. Occurrence and polymorphic transformation. *J. Am. Oil Chem. Soc.* **68**: 710–715.
- Kodali, D. R., D. Atkinson, T. G. Redgrave, and D. M. Small. 1987. Structure and polymorphism of 18-carbon fatty acyl triacylglycerols: effect of unsaturation and substitution in the 2-position. *J. Lipid Res.* **28**: 403–413.
- Engstrom, L. 1992. Triglyceride systems forming molecular compounds. *J. Fat Sci. Technol.* **94**: 173–181.
- Goto, M., K. Honda, L. Di, and D. M. Small. 1995. Crystal structure of a mixed chain diacylglycerol, 1-stearoyl-3-oleyl-glycerol. *J. Lipid Res.* **36**: 2185–2190.
- Di, L., and D. M. Small. 1993. Physical behavior of the mixed chain diacylglycerol, 1-stearoyl-2-oleyl-*sn*-glycerol: difficulties in chain packing produce marked polymorphism. *J. Lipid Res.* **34**: 1611–1623.
- Yoshimoto, N., T. Nakamura, M. Suzuki, and K. Sato. 1991. Phase properties of binary mixtures of petroselinic acid/oleic acid and asclepic acid/oleic acid. *J. Phys. Chem.* **95**: 3384–3390.
- Inoue, T., I. Motoda, N. Hiramatsu, M. Suzuki, and K. Sato. 1993. Phase behavior of binary mixture of palmitoleic acid (*cis*-9-hexadecenoic acid) and asclepic acid (*cis*-11-octadecenoic acid). *Chem. Phys. Lipids* **66**: 209–214.
- Koyano, T., I. Hachiya, and K. Sato. 1992. Phase behavior of mixed systems of SOS and OSO. *J. Phys. Chem.* **96**: 10514–10520.
- Minato, A., S. Ueno, J. Yano, Z. H. Wang, H. Seto, Y. Amemiya, and K. Sato. 1996. Synchrotron radiation X-ray diffraction study on phase behavior of PPP-POP binary mixtures. *J. Am. Oil Chem. Soc.* **73**: 1567–1572.
- Minato, A., S. Ueno, K. Smith, Y. Amemiya, and K. Sato. 1997. Thermodynamic and kinetic study on phase behavior of binary mixtures of POP and PPO forming molecular compound systems. *J. Phys. Chem. B* **101**: 3498–3505.

31. Minato, A., S. Ueno, J. Yano, K. Smith, H. Seto, Y. Amemiya, and K. Sato. 1997. Thermal and structural properties of *sn*-1,3-dipalmitoyl-2-oleoylglycerol and *sn*-1,3-dioleoyl-2-palmitoylglycerol binary mixtures examined with synchrotron radiation X-ray diffraction. *J. Am. Oil Chem. Soc.* **74**: 1213–1220.
32. de Jong, S., T. C. van Soest, and M. A. van Schaick. 1991. Crystal structures and melting points of unsaturated triacylglycerols in the β phase. *J. Am. Oil Chem. Soc.* **68**: 371–378.
33. Larsson, K. 1972. Molecular arrangement in glycerides. *Fette Seifen Anstrichm.* **74**: 136–142.
34. Yano, J., S. Ueno, K. Sato, T. Arishima, N. Sagi, F. Kaneko, and M. Kobayashi. 1993. FT-IR study of polymorphic transformations in SOS, POP, and POS. *J. Phys. Chem.* **97**: 12967–12973.
35. Minato, A., J. Yano, S. Ueno, K. Smith, and K. Sato. 1997. FT-IR study on microscopic structures and conformations of POP-PPO and POP-OPO molecular compounds. *Chem. Phys. Lipids.* **88**: 63–71.
36. Jones, R. N., A. F. McKay, and R. G. Sinclair. 1952. Band progressions in the infrared spectra of fatty acids and related compounds. *J. Am. Chem. Soc.* **74**: 2575–2578.
37. Primas, H., and Hs. H. Gunthard. 1955. Theorie der intensitäten der schwingungsspektren von kettenmolekeln. I. Allgemeine theorie der berechnung von intensitäten der infrarotspektren von grossen molekeln. *Helv. Chem. Acta.* **38**: 1254–1262.
38. Primas, H., and Hs. H. Gunthard. 1953. Die infrarotspektren von kettenmolekeln der formel $R'CO(CH_2CH_2)_nCOR''$. II. Die normalschwingungen des symmetriertypus B_u . *Helv. Chem. Acta.* **36**: 1791–1803.
39. Tasumi, M., T. Shimanouchi, A. Watanabe, and R. Goto. 1964. Infrared spectra of normal higher alcohols—I. *Spectrochimica Acta.* **20**: 629–666.
40. Fichmeister, I. 1974. Infrared absorption spectroscopy of normal and substituted long-chain fatty acids and esters in the solid state. *Prog. Chem. Fats Other Lipids.* **24**: 91–162.
41. Ruig, W. G. 1977. Infrared spectra of diacid and triacid triglycerides. *Appl. Spectrosc.* **31**: 122–131.
42. Amey, R. L., and D. Chapman. 1984. Infrared spectroscopic studies of model and natural biomembranes. In *Biomembrane Structure and Function, Topics in Molecular and Structural Biology*. Vol. 4. D. Chapman, editor. Weinheim, Basel. 199–256.
43. Yano, J., F. Kaneko, M. Kobayashi, and K. Sato. 1997. Structural analyses of triacylglycerol polymorphs with FT-IR techniques: I. Assignments of CH_2 progression bands of saturated monoacid triacylglycerols. *J. Phys. Chem. B.* **101**: 8112–8119.
44. Yano, J., F. Kaneko, M. Kobayashi, D. R. Kodali, D. M. Small, and K. Sato. 1997. Structural analyses of triacylglycerol polymorphs with FT-IR techniques: II. β' -form of 1,2-dipalmitoyl-3-myristoyl-*sn*-glycerol. *J. Phys. Chem. B.* **101**: 8120–8128.
45. Heibert, G. L., and D. F. Hornig. 1952. A new tool for the study of crystalline spectra. *J. Chem. Phys.* **20**: 918–919.
46. Tasumi, M., and S. Krimm. 1968. Vibrational analysis of chain folding in polyethylene crystals. *J. Polym. Sci.* **6**: 995–1010.
47. Spell, S. J., D. M. Sadler, and A. Keller. 1980. Chain trajectory in solution grown polyethylene crystals: correction between infra-red spectroscopy and small-angle neutron scattering. *Polymer.* **21**: 1121–1128.
48. Bentley, P. H., and W. McCrae. 1970. An efficient synthesis of symmetrical 1,3-diglycerides. *J. Org. Chem.* **35**: 2082–2083.
49. Allara, D. L., and J. D. Swalen. 1982. An infrared reflection spectroscopy study of oriented cadmium arachidate monolayer films on evaporated silver. *J. Phys. Chem.* **86**: 2700–2704.
50. Rabolt, J. F., F. C. Burns, N. E. Schlotter, and J. D. Swalen. 1983. Anisotropic orientation in molecular monolayers by infrared spectroscopy. *J. Chem. Phys.* **78**: 946–952.
51. Kaneko, F., H. Miyamoto, and M. Kobayashi. 1996. Polarized infrared attenuated total reflection spectroscopy for three-dimensional structural analysis on long-chain compounds. *J. Chem. Phys.* **105**: 4812–4822.
52. Snyder, R. G. 1960. Vibrational spectra of crystalline *n*-paraffins part I. Methylene rocking and wagging modes. *J. Mol. Spectrosc.* **4**: 411–434.
53. Snyder, R. G. 1967. A revised assignment of the B_{2g} methylene wagging fundamental of the planar polyethylene chain. *J. Mol. Spectrosc.* **23**: 224–228.
54. Knoop, E., and E. Samhammer. 1961. Röntgenographische untersuchungen uber die kristallstruktur einiger triglyceride. *Milchwissenschaft.* **16**: 201–209.
55. de Jong, S., and T. C. van Soest. 1978. Crystal structures and melting points of saturated triglycerides in the β -2 phase. *Acta Crystallogr.* **B34**: 1570–1583.
56. Larsson, K. 1964. The crystal structure of the β -form of trilaurin. *Ark. Kemi.* **23**: 1–15.
57. Jensen, L. H., and A. J. Mabis. 1966. Refinement of the structure of β -tricaprin. *Acta Crystallogr.* **21**: 770–781.
58. Jackson, F. L., and E. S. Lutton. 1950. The polymorphism of certain behenyl mixed triglycerides. A new metastable crystalline form of triglycerides. *J. Am. Oil Chem. Soc.* **27**: 4519–4521.
59. Kobayashi, M. 1988. Vibrational spectroscopic aspects of polymorphism and phase transition of fats and fatty acids. In *Crystallization and Polymorphism of Fats and Fatty Acids*. N. Garti and K. Sato, editors. Marcel Dekker, New York. 139–187.
60. Abrahamsson, S., B. Dahlen, H. Lofgren, and I. Pascher. 1978. Lateral packing of hydrocarbon chains. *Prog. Chem. Fats Other Lipids.* **16**: 125–143.
61. Snyder, R. G., M. C. Goh, V. J. P. Srivatsavoy, H. L. Strauss, and D. L. Dorset. 1992. Measurement of the growth kinetics of microdomains in binary *n*-alkane solid solutions by infrared spectroscopy. *J. Phys. Chem.* **96**: 10008–10019.
62. Arishima, T., K. Sugimoto, R. Kiwata, H. Mori, and K. Sato. 1996. ¹³C cross-polarization and magic-angle spinning nuclear magnetic resonance of polymorphic forms of three triacylglycerols. *J. Am. Oil Chem. Soc.* **73**: 1231–1236.
63. Doucet, J., I. Denicolo, A. Craievich, and A. Collet. 1981. Evidence of a phase transition in the rotator phase of the odd-numbered paraffins $C_{23}H_{48}$ and $C_{25}H_{52}$. *J. Chem. Phys.* **75**: 5125–5127.
64. Ungar, G. 1983. Structure of rotator phases in *n*-alkanes. *J. Phys. Chem.* **87**: 689–695.
65. Sirota, E. B., H. E. King, Jr., D. M. Singer, and H. H. Shao. 1993. Rotator phases of the normal alkanes: an X-ray scattering study. *J. Chem. Phys.* **98**: 5809–5824.
66. Sato, K. 1988. Crystallization and polymorphism transformation. In *Crystallization and Polymorphism of Fats and Fatty Acids*. N. Garti and K. Sato, editors. Marcel Dekker, New York. 3–7.